Cortico-striatal synaptic plasticity underlying compulsive reward seeking

Masaya Harada[1], Agnes Hiver[1], Vincent Pascoli[1] and Christian Lüscher[1,2]

[1]Department of Basic Neurosciences, University of Geneva, Rue Michel-Servet 1, 1206 Geneva, Switzerland,

[2]Service de Neurologie, Department of Clinical Neurosciences, Geneva University Hospital, Rue Gabrielle-Perret-Gentil 4, 1205 Geneva, Switzerland.

Abstract

Loss of control over drug intake and persistent drug-seeking despite negative consequences define addiction. Increase dopamine levels in the mesolimbic system may constitute the initial trigger. Optogenetic self-stimulation of VTA DA neurons (oDASS) has thus been proposed as an addiction model. Indeed, lever pressing to turn on a laser aimed at ChR2 expressing DA neurons is strongly reinforcing. Clinical observations indicate that drug-seeking even with the risk of harmful consequences occurs only in a fraction of users, with chronic drug consumption. Here, mice carried out a seek-take chain in order to selectively study compulsive seeking behavior. Once fully established, a probabilistic punishment of the seeking lever led to the emergence of two classes of mice; those that persevered and those that renounced oDASS. *Ex vivo* characterization of three distinct cortico-striatal streams demonstrated a selective potentiation of excitatory synapses of the orbito-frontal cortex (OFC) to dorsal striatum projection in persevering mice. Taken together, our data indicate a gain-of-function of OFC striatal control in compulsive oDASS.

Introduction

Clinical observations indicate that addiction is not limited to compulsive drug use. Addicts are preoccupied with procuring drugs for subsequent use and deploy much effort seeking the drug, even in the light of a high risk of personal, physical and social harm. As a matter of fact, compulsive seeking is maximal once the drug is no longer available and will not stop even in the light of major adverse consequences. The distinction between compulsive drug use and compulsive drug seeking has been modeled in rodents, using a seek-take chain paradigm (Pelloux et al., 2007). In brief, the animals learn to press a seeking lever during an interval of random period, which when completed leads to the presentation of a taking lever that allows drug access.

The transition to compulsion is observed only in some individuals and not others. This holds true for humans (Wagner and Anthony, 2002) as well as rodents (Deroche-Gamonet and Piazza, 2014). With repetitive consumption, a bimodal distribution of behavior emerges, where some individuals continue to seek and self-administer the drug even when facing harmful consequences, while others will renounce.

A leading hypothesis posits that cortico-striatal projections control this transition, as more and more dorsal parts of striatum are recruited (Everitt and Robbins, 2016). An imbalance of neural systems underlying habit and goal-directed action may underlie compulsive drug seeking (Vandaele and Janak, 2017) as with prolonged self-administration (SA), rats become insensitive to devaluation of the taking lever (Zapata et al., 2010). This implicates the dorsolateral striatum, which when silenced, led to a switch back to a goal-directed behaviour (Zapata et al., 2010). Compulsive SA may also reflect a deficit of inhibitory control, where drug seeking despite punishment persists due to the hypofunction of mPFC (Chen et al., 2013). By contrast, we have found a hyperactivity of the OFC to DS projection in mice complusively self-stimulating VTA DA neurons (Pascoli et al., 2018; 2015), suggesting a decision making bias favoring reward pursuit despite the risk of punishment.

Top down control of specific parts of the prefrontal cortex may thus control compulsion. To parse their relative contribution, we developed a mouse model of compulsive oDASS seeking, using a heterogeneous seek-take schedule and measured synaptic plasticity at identified cortico-striatal pathways.

Methods

Animals.
Mice (age 8–24 weeks) were heterozygous BAC-transgenic mice in which the Cre-recombinase expression was under the control of the regulatory elements of the dopamine transporter gene (DAT-Cre mice). Dat-Cre mice were originally provided by G. Schutz and only heterozygous mice were used for experiments. DAT B6.SJL-Slc6a3tm1.1(cre)Bkmn/J (also known as DAT-IRES-Cre) mice were also used. Weights and genders were distributed homogeneously among the groups. Transgenic mice had been backcrossed into the C57BL/6 line for a minimum of four generations. All animals were kept in a temperature- and humidity-controlled environment with an inverted 12-h light/12-h dark cycle (lights on at 7PM). All procedures were approved by the Institutional Animal Care and Use Committee of the University of Geneva and by the animal welfare committee of the Cantonal of Geneva, in accordance with Swiss law.

Stereotaxic injections.
AAV5-EF1a-DIO-ChR2(H134R)-eYFP produced at the University of North Carolina (UNC Vector Core Facility) were injected into the VTA. Anaesthesia was induced at 2% and maintained at 1.0% isoflurane (w/v) (Baxter) during surgery. The mouse was placed in a stereotaxic frame (Angle One) and craniotomies were performed using stereotaxic coordinates (for VTA: anterior–posterior (AP) −3.3; medial–lateral (ML) −0.9 with a 10° angle; dorsal–ventral (DV) −4.28). Injections of virus (0.7 µl) used graduated pipettes (Drummond Scientific), broken back to a tip diameter of 10–15 mm, at an infusion rate of 0.05 µl min−1. Following the same procedure, AAV8-hSyn-ChrimsonR-tdTomato (UNC), (Duke University) was injected bilaterally in the mPFC (AP +1.9; ML ±0.3; DV −2.5), OFC (AP +2.6; ML ±1.75; DV −1.95) or M1 (AP +1.1; ML ±1.7; DV −1.75). During the same surgical procedure, a unique chronically indwelling optic fibre cannula was implanted above the VTA using the exact same coordinates as for the injection except for DV coordinate, which was reduced to 4.18. Two screws were fixed into the skull to support the implant, which was further secured with dental cement. The first behavioural session typically occurred 10−14 days after surgery to allow sufficient expression of ChR2.

Optogenetic self-stimulation apparatus.
Mice infected with ChR2 in the VTA were placed during their dark phase in operant chambers (ENV-307A-CT, Med Associates) situated in a sound-attenuating box (Med Associates). The optic fibre of the mouse was connected to DPSS blue-light lasers (CNI-473-140-10-LED-TTL1-MM200FC; Laser 2000) via a FC/PC fibre cable (M72L02; Thorlabs) and a simple rotary joint (FRJ-FC-FC; Doric Lenses) allowing free movement during operant behaviour. Power at the exit of the patch cord was set to 15 ± 1 mW. Two retractable levers were present on one wall of the chamber and a cue light was located above each lever. A rack mount interface cabinet (SG-6010A, Med Associates) containing a programmable constant current shocker (ENV-413, Med Associates) connected to a quick disconnect grid harness (ENV-307A-QD, Med Associates) was used to provide foot shocks during punishment sessions. The apparatus was controlled and data captured using MED-PC IV software (Med Associates).

Acquisition of taking response.
In this first phase of training, each session started with the presentation of the taking lever (left/right, counterbalanced), which then is never retracted during the session. A single press on the taking lever (FR1) resulted in a 10-s illumination of a cue light (pulses of 1 s at 1 Hz). After a delay of 5 s, onset of a 15-s laser stimulation (473 nm) composed of 30 bursts separated by 250 ms (each burst consisted of 5 laser pulses of 4-ms pulse width at 20 Hz). A 20-s time-out followed the rewarded lever press, during which lever presses had no consequences but were still recorded. Each of the 5 daily acquisition sessions lasted 120 min or until the mouse reached 80 optogenetic stimulations, whichever came first.

Training of the seek-take chain.
During this second phase, mice learned the seek-take chain with an FR1. Each trial of the seek-take chained schedule began with the presentation of the seeking lever (opposite to the taking lever), with the taking lever retracted. A single press on the seeking lever resulted in the retraction of the seeking lever and presentation of the taking lever. A single press on the taking lever resulted in the delivery of the cue light, laser stimulation, and retraction of the taking lever. After a 5s time-out, another trial started with a novel presentation of the seeking lever. Daily session lasted 120 min or until the mouse reached 80 optogenetic stimulations, whichever came first. Mice underwent 7 sessions of FR1 seek-take chained schedule, and then a random interval (RI) schedule was introduced.
During the RI schedule, each trial started with the presentation of the seeking lever, with the taking lever retracted. The first press on the seeking lever initiated the RI schedule. Seeking lever presses during RI had no programmed consequences but are still recorded. The first seeking lever press after the end of the RI resulted in the retraction of the seeking lever and the presentation of the taking lever. A single press on the taking lever resulted in the delivery of the cue light, laser stimulation and the retraction of the taking lever. Following a 5s time-out, the seeking lever presentation initiated another trial. Three RI parameters were used: RI5 (0.5s, 5s or 10s), RI30 (15s, 30s or 45s) and RI60 (45s, 60s or 75s). Mice underwent 3 sessions for each RI. Sessions lasted 360 min or until the mouse reached 80, 60 or 40 optogenetic stimulations, whichever came first, for respectively RI5, 30 or 60.

Evaluation of compulsivity.
After the training, mice underwent additional sessions of RI60 schedule. Stable performance (earning all 30 stimulations) across four consecutive sessions served as a baseline before the punishment sessions. During punishment sessions, for 30% of the trials, the first seeking lever press after RI resulted in the retraction of the seeking lever and the delivery of the mild foot shock (0.25mA, 500ms) and led to the time-out period directly without the presentation of the taking lever. The remaining 70% trials contained no punishment, but resulted as previously in the presentation of the taking lever. Mice were given 5 punishment sessions. During baseline and punishment sessions, mice had 7 min to finish each trial. After a failed trial, a novel seeking lever presentation is given.

Slice electrophysiology.
Whole-cell patch-clamp recordings of striatal neurons were performed 24 h after the last punished session or in slices from naive mice. The AMPAR/NMDAR ratio was calculated at +40 mV with the AMPAR component pharmacologically isolated using D-AP5 (50 μM) and the NMDAR EPSC component was determined by subtraction. Currents were evoked with optogenetic stimulation on slices of mPFC,OFC or M1 terminals infected with Chrimson. Coronal 230-μm slices of mouse brain were prepared in cooled artificial cerebrospinal fluid containing (in mM): NaCl 119, KCl 2.5, MgCl 1.3, CaCl2 2.5, Na2HPO4 1.0, NaHCO3 26.2 and glucose 11, bubbled with 95% O2 and 5% CO2. Slices were kept at 32–34 °C in a recording chamber superfused with 2.5 ml min−1 artificial cerebrospinal fluid.
Ex vivo synaptic properties of the striatum.
Visualized whole-cell patch-clamp recording techniques were used to measure synaptic responses to optogenetic stimulation of mPFC,OFC or M1 terminals. The holding potential was −70 mV and the access resistance was monitored by a hyperpolarizing step of −14 mV. The liquid junction potential was small (−3 mV), and therefore traces were not corrected. Experiments were discarded if the access resistance varied by more than 20%. Currents were amplified (Multiclamp 700B, Axon Instruments), filtered at 5 kHz and digitized at 20 kHz (National Instruments Board PCI-MIO-16E4, Igor, Wave Metrics). For recordings of optogenetically evoked EPSCs, the internal solution contained (in mM): CsCl 130, NaCl 4, creatine phosphate 5, MgCl2 2, NA2ATP 2, NA3GTP 0.6, EGTA 1.1, HEPES 5 and spermine 0.1. QX-314 (5 mM) was added to the solution to prevent action currents. Synaptic currents were evoked by short light pulses (4 ms) at 0.1 Hz through an LED (PE-100, cool-LED) placed through the objective above the tissue. To isolate AMPAR-evoked EPSCs the NMDA antagonist d-2-amino-5-phosphonovaleric acid (D-AP5, 50 μM) was applied to the bath. The NMDAR component was calculated as the difference between the EPSCs measured in the absence and in the presence of D-AP5. The AMPAR/NMDAR ratio was calculated by dividing the peak amplitudes. The rectification index of AMPAR was calculated as the ratio of the chord conductance calculated at negative potential divided by chord conductance at positive potential. Examples traces are averages of 10–15 sweeps. All experiments were performed in the presence of picrotoxin (100 μM).

Tissue preparation for imaging.
Mice were anaesthetized with pentobarbital (300 mg/kg, intraperitoneally, Sanofi-Aventis) and transcardially perfused with 4% (w/v) paraformaldehyde in PBS (pH 7.5). Brains were post-fixed overnight in the same solution and stored at 4 °C. Coronal sections (50-mm thick) were cut with a vibratome (Leica), stained with Hoechst (Sigma- Aldrich) and mounted with Mowiol (Sigma-Aldrich). Full images of brain slices were obtained with a Zeiss Axioscan Z1 system equipped with a Plan-Apochromat 10×/0.45 NA objective, together with filters for 4′,6-diamidino-2-phenylindole (DAPI) (emission band-pass filter: 445/50 nm), enhanced green fluorescent protein (eGFP) (emission band-pass filter: 525/50 nm) and cyanine 3 (Cy3) (emission band- pass filter: 605/70 nm).
Images from VTA and striatum were obtained using sequential laser scanning confocal microscopy (Zeiss LSM800). Photomicrographs were obtained with the following band-pass and long-pass filter settings: UV excitation (band-pass filter: 365/12 nm), GFP (band-pass filter: 450−490 nm), Cy3 (band-pass filter: 546/12 nm) and Cy5 (band-pass filter: 546/12 nm). For biocytin (Sigma-Aldrich, B4261) staining, streptavidin–Cy5 (Invitrogen 434316) was used. For immunohistochemistry, the following primary antibody (rabbit polyclonal anti-tyrosine hydroxylase, Millipore AB152, lot 2722866, diluted 1:500) and the secondary antibody (donkey anti-rabbit Cy3, Millipore AP182C, lot 2397069, diluted 1:500) were used.

Results

A subpopulation of mice develops compulsive oDASS seeking.

DAT-Cre mice were injected with an AAV5-EF1a-DIO-channelrhodopsin-2 (ChR2)-eYFP bilaterally into the VTA and implanted with an optic fiber above the injection site (Figure 1A). ChR2 expression is observed exclusively in TH (tyrosine

hydroxylase) positive neurons, showing the specificity of the DAT-Cre mouse line for targeting dopamine neurons of the VTA. Acquisition of self-stimulation started 12-14 d after surgery to allow recovery and virus expression. Acquisition consisted in 5 sessions of FR1 with only the taking lever, 16 sessions of seek-take chain schedule with increasing random interval (RI from 0, 5, 30 to 60 s). After the training with only the taking lever, a heterogeneous seeking-taking chain schedule was introduced, during which mice had to press on a second lever, called seeking lever in order to obtained the taking lever presentation (Fig 1B, see methods for details). When the mouse pressed the taking lever, the optogenetic stimulation (30 bursts of 5 pulses of 4 ms at 20 Hz) was delivered with a delay of 5 s (Figure 1C). After acquisition of the seek-take chain, mice had a stable performance under RI60 and they all completed the 30 trials during for 4 daily sessions of baseline. During baseline sessions, the first seeking lever press after a RI60 (45, 60 or 75 s) triggered the presentation of the taking lever, which when pressed turned on the laser. Then mice underwent 5 d of punished sessions, during which a foot-shock (0.25 mA, 500 ms) was delivered at the first press on the seeking lever after the end of the RI in 30% of the trials (Figure 1B), while 70 % of the trial led to the presentation of the taking lever. During baseline sessions, all the mice completed the 30 trials but during the punished sessions, some mice failed to complete the 30 trials (Figure 1D and E). Some mice made less than 20 trials during the last two sessions of punishment while other mice were still able to complete more than 24 trials during punished sessions. Using unsupervised classification method, with several behavioral parameters (number of seeking press, completed trials and session duration), two distinct groups of mice were found (Figure 1F). About 40 % of the tested mice were assigned to a first group that drastically reduced their seek-take chain performance under punishment, called renouncers. The second group, called perseverer, is made of 60 % of the mice that kept a high rate of seeking presses under punishment and completed most the trials (Figure 1E and F). The number of seeking lever presses made during the baseline sessions was not different between the two groups and could not predict perseverance under punishment (Figure 1G). Overall, the number of completed trials was significantly reduced during punished sessions in renouncers but not in perseverers.

Distinct cortico-striatum pathways

Specific cortical areas connect to defined sub-regions of the DS (Hunnicutt et al., 2016). To characterize distinct cortico-striatal pathways in mice, the retrograde tracer CTB was injected in the medial, central and lateral part of the dorsal striatum of the same mice, using dyes of different color linked to CTB (Figure 2 A and B). We found

that neurons in the medial prefrontal cortex, especially within the prelimbic cortex were stained almost exclusively with the CTB-488 seeded in the mDS (Figure 2C and D). By contrast, OFC was mostly labeled with CTB-555 that was injected in the central part of the dorsal striatum (Figure 2E and F). Few neurons in the OFC were found to project to the lateral DS. In the motor cortex (M1) we found a high number of neurons stained with the CTB-647 that was injected in the lateral DS (Figure 2 G and H). Despite a small proportion of neurons with divergent output from their cortical area, these data confirm that sub-regions of the DS mostly receive specific cortical inputs. This indicates that the three parallel streams can be targeted anterogradely by injecting AAV8-Syn-ChrimsonR in mPFC, OFC or M1 in order to test synaptic plasticity at different synapses (mPFC-mDS, OFC-cDS and M1-lDS).

Transmission at cortico-striatal synapses in compulsive mice

To evaluate whether the state of the three synapses in correlation with the compulsive oDASS seeking, we injected an adeno associated virus carrying the construct of the red-shifted excitatory opsin (ChrimsonR) either in the mPFC, OFC or M1 of DAT-cre mice infected with ChR2 in the VTA (Figure 3 A, C and E). Mice were then submitted to the oDASS seeking-taking schedule until determination of their compulsivity. Next, to probe for synaptic adaptation underlying compulsive behavior, we performed *ex vivo* recordings in acute slices from persevering and renouncing mice, 24 h after the last punished session. Excitatory transmission was evoked by short light pulses (4 ms), using an LED. EPSCs were recorded from the medial, central or lateral part of the DS. To compare synaptic strength in the 2 groups of mice at each of the 3 synapses, the AMPAR-EPSCs to NMDAR-EPSCs ratio (A/N) was determined at positive potential with pharmacological isolation of the AMPAR-EPSCs component with AP5. A/N was also measured in slices from naïve mice at the 3 synapses. At mPFC-mDS and M1-lDS, we found no difference in A/N in persevering or renouncing mice when compared to naïve mice (Figure 3 B and F). By contrast, the A/N at OFC-cDS was higher in slices from persevering mice than in slices from renouncing or naïve mice (Figure 3D). Of note, the A/N ratio was smaller at M1-lDS than other synapses in the DS. Taken-together these data demonstrate that synaptic strength was increased in compulsive mice at OFC-cDS but not at mPFC-mDS or M1-lDS. These results suggest that compulsive oDASS seeking tested in a seek-take chain schedule could be mediated by OFC-cDS plasticity as it was shown in a version of the oDASS in which the active lever was punished (Pascoli et al., 2018).

Discussion

Here, we observed the emergence of compulsive behaviour in a seek-take chain of oDASS, which was associated with a selective strengthening of the OFC to central DS projection.

In previous studies, including our own (Pascoli et al., 2015; 2018), punishment was delivered at the same lever as the reward within a few seconds. One could therefore argue that the punishment became a predictive-cue. A seek-take chain with punishment at the seeking lever hedges for this possibility. Compulsive seeking and compulsive taking may be mediated by distinct system, which is suggested by the different sensitivity when the punishment is given at seeking or taking press (Pelloux et al., 2014). However, in this study, no distinct subpopulations of rats emerged, and the ratio of addicted animals remains to be determined. By contrast, using the same seek-take chain paradigm, we found a similar ratio of persevering mice that the one obtained when the taking lever was punished (Pascoli et al., 2018).

There is an agreement that compulsion is controlled by top down, cortico-striatal projections. Different cortical regions project to different sub-regions of the striatum (Hunnicutt et al., 2016), which we confirmed here with the identification of three distinct streams (mPFC to mDS, OFC to central DS and M1 to dlDS). The nature and sequence of adaptations in these streams however is subject to intense research, and it remains elusive whether gain or loss of function predominates. For example, the potentiation of mPFC-mDS was causally linked to alcohol consumption (Ma et al., 2018), while several clinical (Goldstein and Volkow, 2011) and preclinical studies (Chen et al., 2013) revealed a hypofunction of mPFC in addicts.

Here, synaptic transmission in the mPFC-mDS pathway remained unaltered with compulsive oDASS seeking. Maybe the mPFC to NAc controls behavioral inhibition at this stage. D2-receptors in NAc core are indeed necessary in an active avoidance task (Danjo et al., 2014) and addicted patients have lower expression level of the dopamine D2 receptor (Volkow et al., 2008). One explanation of compulsive seeking might therefore result from a deficit of inhibitory control, which could come from a lack of aversive learning.

Another explanation of compulsivity is an imbalance of goal-directed and habitual behaviour (Everitt and Robbins, 2016; 2013; 2005; Vandaele and Janak, 2017). It has been proposed that an abnormal habit formation is underlying compulsive drug

seeking. For example it has been shown that the lateral part of the dorsal striatum is involved in habitual cocaine self-administration (Zapata et al., 2010). Moreover, silencing of the lateral DS with pharmacology attenuated compulsivity (Jonkman et al., 2012). In the present study, compulsive oDASS was observed in the presence of normal M1 to lDS transmission, challenging the need of habit formation in compulsion. Moreover, to the best of our knowledge, there is no direct evidence showing that compulsive animals form stronger habits than non-compulsive ones. In a puzzle solving task, requiring a strong goal-directed behavior (Singer et al., 2017) some rats still showed addiction-like behaviour. Compulsivity may thus be considered as an extreme form of goal-directed behaviour.

Could the strengthing of the OFC to DS projection be the correlate of excessive goal-directed behavior? Activity in the OFC encodes expected value of an action (Takahashi et al., 2013), a function that is disrupted after prolonged exposure to an addictive drug (Lucantonio et al., 2015). Maybe there is an overestimation of the value of the drug in compulsive individuals, explaining perseverance of drug seeking despite punishment. In this model, the gain of function in the OFC leads to a potentiation of a specific striatal projection that eventually underlies compulsive drug seeking. Comparisons of different model need to take into account the stage of disease. The OFC gain of function may represent an intermediate state promoting further drug use before the irreversible end-stage disease, where a hypometabolism of the cortex dominates, and where deficits in cognitive and executive functioning are prevalent in addicts. Targeting the OFC hyperactivity may therefore represent a crucial step in the treatment of early drug addiction.

References

Chen, B.T., Yau, H.-J., Hatch, C., Kusumoto-Yoshida, I., Cho, S.L., Hopf, F.W., Bonci, A., **2013**. Rescuing cocaine-induced prefrontal cortex hypoactivity prevents compulsive cocaine seeking. *Nature 496, 359-362. doi:10.1038/nature12024*

Danjo, T., Yoshimi, K., Funabiki, K., Yawata, S., Nakanishi, S., **2014**. Aversive behavior induced by optogenetic inactivation of ventral tegmental area dopamine neurons is mediated by dopamine D2 receptors in the nucleus accumbens. *Proceedings of the National Academy of Sciences of the United States of America 111, 6455–6460. doi:10.1073/pnas.1404323111*

Deroche-Gamonet, V., Piazza, P.V., **2014**. Psychobiology of cocaine addiction: Contribution of a multi-symptomatic animal model of loss of control. *Neuropharmacology 76, 437–449. doi:10.1016/j.neuropharm.2013.07.014*

Everitt, B.J., Robbins, T.W., **2016**. Drug Addiction: Updating Actions to Habits to Compulsions Ten Years On. Annual Review of Psychology *67, 23–50. doi:10.1146/annurev-psych-122414-033457*

Everitt, B.J., Robbins, T.W., **2013**. From the ventral to the dorsal striatum: Devolving views of their role in drug addiction. *Neuroscience & Biobehavioral Reviews 37, 1946–1954. doi:10.1016/j.neubiorev.2013.02.010*

Everitt, B.J., Robbins, T.W., **2005**. Neural systems of reinforcement for drug addiction: from actions to habits to compulsion. *Nature Neuroscience 8, 1481–1489. doi:10.1038/nn1579*

Goldstein, R.Z., Volkow, N.D., **2011**. Dysfunction of the prefrontal cortex in addiction: neuroimaging findings and clinical implications. Nature Reviews Neuroscience *12, 652–669. doi:10.1038/nrn3119*

Hunnicutt, B.J., Jongbloets, B.C., Birdsong, W.T., Gertz, K.J., Zhong, H., Mao, T., **2016**. A comprehensive excitatory input map of the striatum reveals novel functional organization. *Elife 5. doi:10.7554/eLife.19103*

Jonkman, S., Pelloux, Y., Everitt, B.J., **2012**. Differential Roles of the Dorsolateral and Midlateral Striatum in Punished Cocaine Seeking. *Journal of Neuroscience 32, 4645–4650. doi:10.1523/JNEUROSCI.0348-12.2012*

Lucantonio, F., Kambhampati, S., Haney, R.Z., Atalayer, D., Rowland, N.E., Shaham, Y., Schoenbaum, G., **2015**. Effects of prior cocaine versus morphine or heroin self-administration on extinction learning driven by overexpectation versus omission of reward. *Biological Psychiatry 77, 912–920. doi:10.1016/j.biopsych.2014.11.017*

Ma, T., Cheng, Y., Hellard, E.R., Wang, X., Lu, J., Gao, X., Huang, C.C.Y., Wei, X.-Y., Ji, J.-Y., Wang, J., **2018**. Bidirectional and long-lasting control of alcohol- seeking behavior by corticostriatal LTP and LTD. *Nature Neuroscience 21, 373–383. doi:10.1038/s41593-018-0081-9*

Pascoli, V., Hiver, A., Zessen, R., Loureiro, M., Achargui, R., Harada, M., Flakowski, J., Lüscher, C., **2018**. S*tochastic synaptic plasticity underlying compulsion in a model of addiction. Nature 564, 366–371. doi:10.1038/s41586-018-0789-4*

Pascoli, V., Terrier, J., Hiver, A., Lüscher, C., **2015**. Sufficiency of Mesolimbic Dopamine Neuron Stimulation for the Progression to Addiction. *Neuron 88, 1054–1600. doi:10.1016/j.neuron.2015.10.017*

Pelloux, Y., Everitt, B.J., Dickinson, A., **2007**. Compulsive drug seeking by rats under punishment: effects of drug taking history. *Psychopharmacology 194, 127–137. doi:10.1007/s00213-007-0805-0*

Pelloux, Y., Murray, J.E., Everitt, B.J., **2014**. Differential vulnerability to the punishment of cocaine related behaviours: effects of locus of punishment, cocaine taking history and alternative reinforcer availability. *Psychopharmacology 232, 125–134. doi:10.1007/s00213-014-3648-5*

Singer, B.F., Fadanelli, M., Kawa, A.B., Robinson, T.E., **2018**. Are cocaine-seeking "habits" necessary for the development of addiction-like behavior in rats? Journal of Neuroscience *38, 60-73. doi:10.1523/JNEUROSCI.2458-17.2017*

Takahashi, Y.K., Chang, C.Y., Lucantonio, F., Haney, R.Z., Berg, B.A., Yau, H.-J., Bonci, A., Schoenbaum, G., **2013**. Neural Estimates of Imagined Outcomes in the Orbitofrontal Cortex Drive Behavior and Learning. *Neuron 80, 507–518. doi:10.1016/j.neuron.2013.08.008*

Vandaele, Y., Janak, P.H., **2017**.. Defining the place in habit in substance use disorder. Progress in Neuro-Psychopharmacology & Biological Psychiatry *87, 22–32. doi:10.1016/j.pnpbp.2017.06.029*

Volkow, N.D., Fowler, J.S., Wang, G.J., Baler, R., Telang, F., **2008**. Imaging dopamine's role in drug abuse and addiction. *Neuropharmacology. 1, 3–8. doi:10.1016/j.neuropharm.2008.05.022*

Wagner, F.A., Anthony, J.C., **2002**. From first drug use to drug dependence; developmental periods of risk for dependence upon marijuana, cocaine, and alcohol. *Neuropsychopharmacology 26, 479–488. doi:10.1016/S0893-133X(01)00367-0*

Zapata, A., Minney, V.L., Shippenberg, T.S., **2010**. Shift from Goal-Directed to Habitual

Cocaine Seeking after Prolonged Experience in Rats. Journal of Neuroscience *30, 15457–15463. doi:10.1523/JNEUROSCI.4072-10.2010*

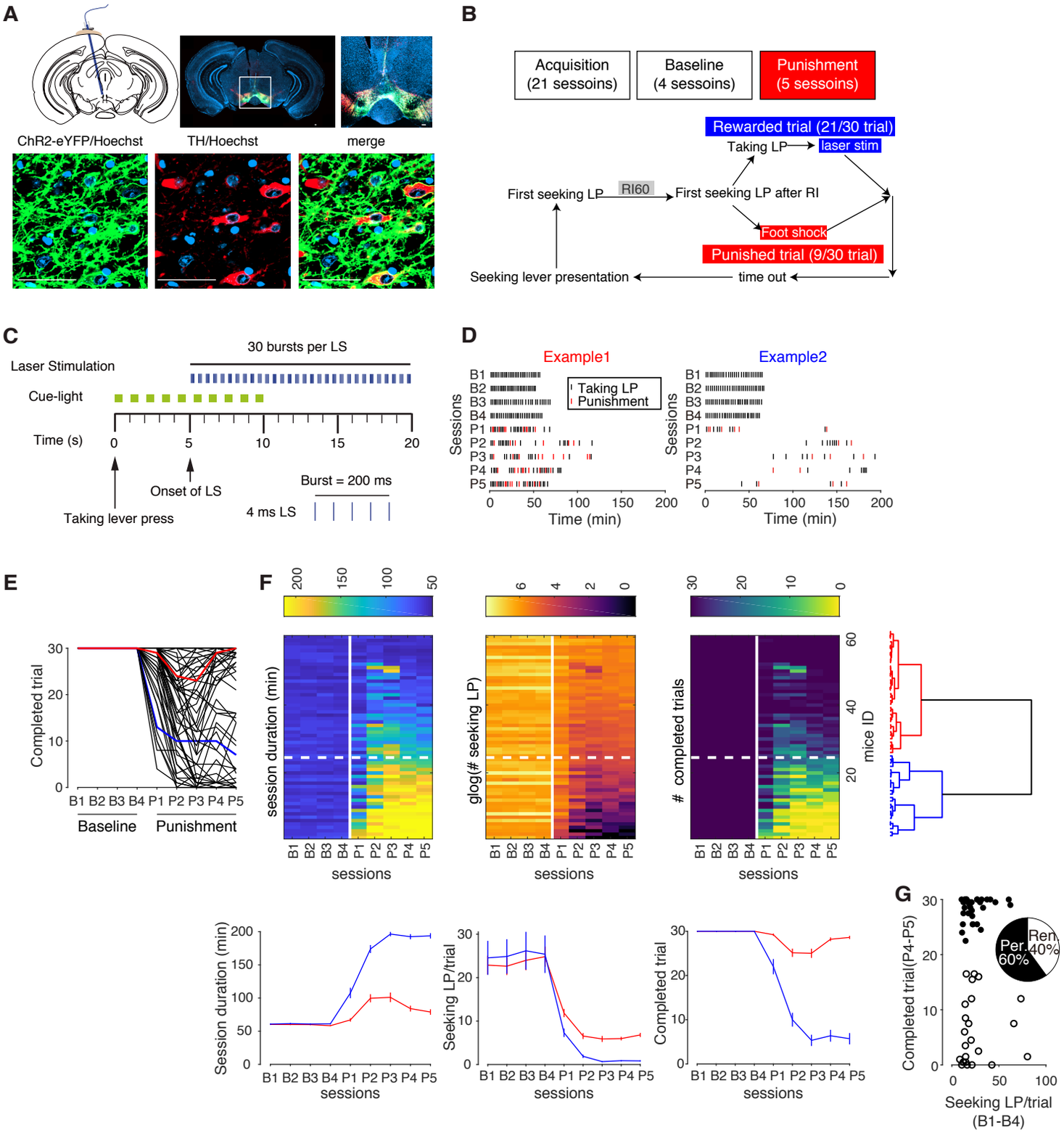

Figure 1. (A)Schematic of optic fiber placement above the VTA (top, left), with coronal image of VTA from a DAT-Cre+ mouse infected with AAV5-DIO-ChR2-eYFP (top, center). Zoom of infected VTA with optic fiber tract (top, right) and co-localization of ChR2-eYFP with tyrosine hydroxylase (TH) expressing neurons (bottom, right). Scale bars, 100 µm. (B) Experimental timeline (Top), and paradigm (Bottom). Details in the method. (C) Press of taking lever triggered a cue light and 5 s later the laser stimulation (LS, 30 bursts composed of 5 short laser pulses, 4-ms width at 20 Hz). (D) Raster plots of 4 days of baseline and 5 days of punishment sessions for a mouse keeping a high completed trial rate during punished sessions (example 1,left) and for a mouse showing a low completed trial rate during punished sessions (example 2,right). (E) Number of completed trials during baseline and punishment sessions (Top). Red and blue lines show the examples of two mice displayed in Panel (D). (F) Hierarchical clustering yielded two sub set of mice (top). Average of each parameter for two populations (bottom). (G) Completed trials as a function of the baseline seeking lever presses.

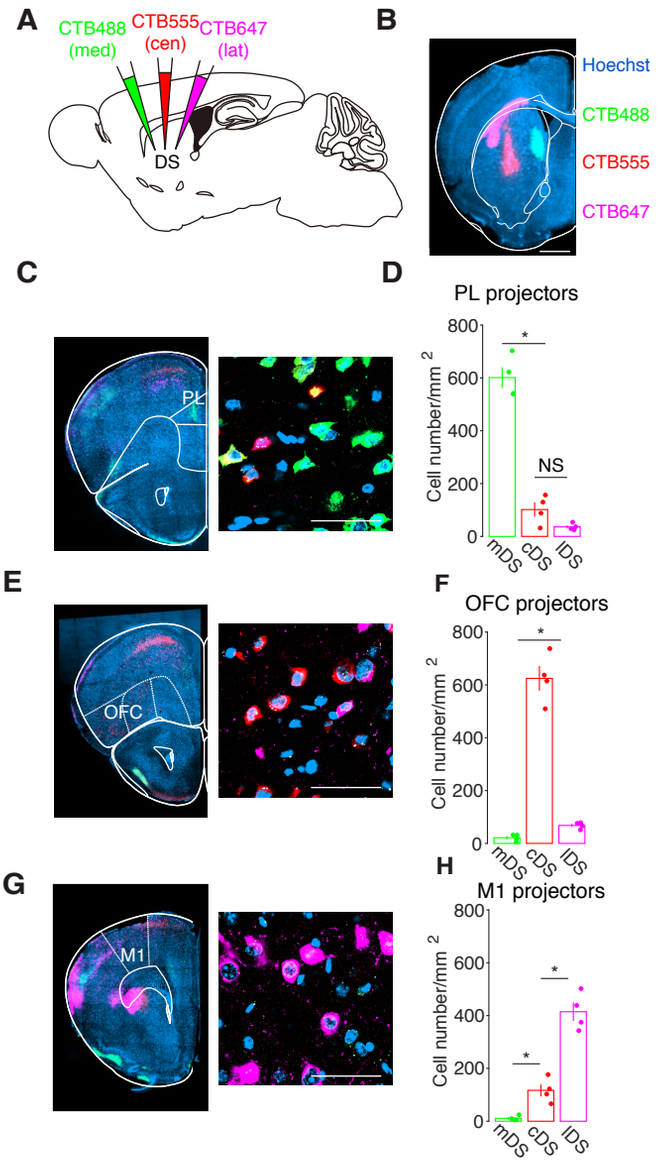

Figure 2. (A) Schematic for the experiment. (B) Retograde tracer, CTB conjugated to the dye Alexa 488 (green), 555(red), or 647 (magenta) were injected in medial, central or lateral part of the dorsal striatum, respectively. (C) Example pictures of low (left) and high (right) magnification of mPFC. (D) Quantification of PL projectors. $F(2,9)=124.4$, $p<0.0001$, Post-hoc comparison with Bonferroni test yielded: $p<0.0001$ for medial versus central; $p<0.0001$ for medial versus lateral. (E) Example pictures of low (left) and high (right) magnification of OFC. (F) Quantification of OFC projectors. $F(2,9)=149.3$, $p<0.0001$, Post-hoc comparison with Bonferroni test yielded: $p<0.0001$ for medial versus central; $p<0.0001$ for central versus lateral. (G) Example pictures of low (left) and high (right) magnification of M1. (H) Quantification of M1 projectors. $F(2,9)=73.11$, $p<0.0001$, Post-hoc comparison with Bonferroni test yielded: $p<0.0001$ for medial versus lateral; $p<0.0001$ for central versus lateral; $p<0.05$ for medial versus central. Scale bars, 50 µm. Error bars, s.e.m.

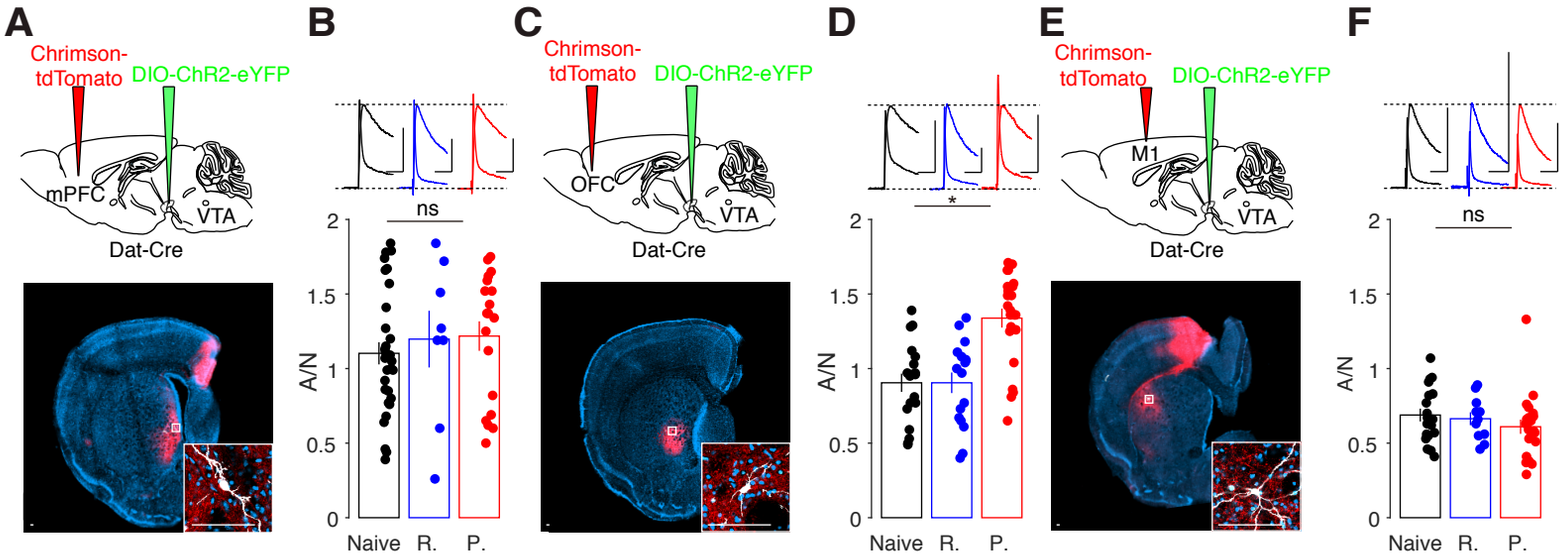

Figure 3. (A) Schematic of the preparation for ex vivo recordings of mPFC–medial part of the dorsal striatum (mDS) synapses (Top). Coronal section shows terminals in the striatum and recorded neuron (bottom). Inset shows recorded neuron at high magnification. (B) Example traces (average of 20 sweeps) AMPA and NMDA-EPSCs, recorded at +40 mV in mDS slices from naive, renouncer or perseverer mice (top). A/N of three groups are not stastically different(bottom) (n=31/8/19, naive/renouncer,F(2,55)=0.46, p=0.63). (C) Schematic of the preparation for ex vivo recordings of OFC–central part of the dorsal striatum (cDS) synapses (Top). Coronal section shows terminals in the striatum and recorded neuron (bottom). Inset shows recorded neuron at high magnification.(D) Example traces (average of 20 sweeps) AMPA and NMDA-EPSCs, recorded at +40 mV in cDS slices from naive, renouncer or perseverer mice (top). A/N is incereased in perseverer mice but not renouncer mice (n=19/17/23,naive/renouncer/perseverer. F(2,56)=15.95, p<0.0001, Post-hoc comparison with Bonferroni test yielded: p<0.0001 for naive versus perseverer; p<0.0001 for renouncer versus perseverer.(E) Schematic of the preparation for ex vivo recordings of M1–lateral part of the dorsal striatum (lDS) synapses (Top). Coronal section shows terminals in the striatum and recorded neuron (bottom). Inset shows recorded neuron at high magnification. (F) Example traces (average of 20 sweeps) AMPA and NMDA-EPSCs, recorded at +40 mV in lDS slices from naive, renouncer or perseverer mice (top). A/N of three groups are not stastically different(bottom) (n=17/11/21, naive/renouncer/perseverer. F(2,46)=1.23, p=0.30). Scale bars, 50 ms, 200 pA, and 100 µm. Error bars, s.e.m.